ISSN 0915-633X

NATIONAL INSTITUTE FOR FUSION SCIENCE

Hydrogen Production in Fusion Reactors

S. Sudo, Y. Tomita, S. Yamaguchi, A. Iiyoshi, H. Momota,
O. Motojima, M. Okamoto, M. Ohnishi, M. Onozuka and
C. Uenosono

(Received – Oct. 8, 1993)

NIFS-253 Nov. 1993

RESEARCH REPORT
NIFS Series

NAGOYA, JAPAN

HYDROGEN PRODUCTION IN FUSION REACTORS

S. Sudo, Y. Tomita, S. Yamaguchi, A. Iiyoshi, H. Momota,
O. Motojima, M. Okamoto, M. Ohnishi*,
M. Onozuka**, C. Uenosono***

National Institute for Fusion Science, Nagoya 464-01, Japan
*Kyoto University, Uji 611, Japan
**Mitsubishi Heavy Industries, Ltd., Minato-ku, Tokyo 105, Japan
***The Kansai Electric Power Co., Inc., Kita-ku, Osaka 530, Japan

[The essential part of this paper was presented at ICENES'93,
Makuhari, Japan, 1993, BP-26.]

KEYWORDS: hydrogen production, fusion reactor, use of
bremsstrahlung, electron-hole pair production
by γ - ray

HYDROGEN PRODUCTION IN FUSION REACTORS

S. Sudo, Y. Tomita, S. Yamaguchi, A. Iiyoshi, H. Momota, O. Motojima, M. Okamoto, M. Ohnishi*, M. Onozuka**, C. Uenosono***

National Institute for Fusion Science, Nagoya 464-01, Japan
*Kyoto University, Uji 611, Japan
**Mitsubishi Heavy Industries, Ltd., Minato-ku, Tokyo 105, Japan
***The Kansai Electric Power Co., Inc., Kita-ku, Osaka 530, Japan

ABSTRACT

As one of methods of innovative energy production in fusion reactors without having a conventional turbine-type generator, an efficient use of radiation produced in a fusion reactor with utilizing semiconductor and supplying clean fuel in a form of hydrogen gas are studied. Taking the candidates of reactors such as a toroidal system and an open system for application of the new concepts, the expected efficiency and a concept of plant system are investigated.

KEYWORDS: hydrogen production, fusion reactor, use of bremsstrahlung, electron-hole pair production by γ - ray,

I. INTRODUCTION

Scientific feasibility of the fusion reactor scheme with using the deuterium - tritium (D-T) fuel cycle will be proved in near future. It seems, however, very difficult to achieve economic feasibility, mainly because 80 % of the D-T fusion energy is in form of 14 MeV neutrons which induce radiation damage and radioactivity in the structure surrounding the plasma. The challenging attempts to minimize such harmful effects by neutrons, of course, have been continued so far. Under the circumstances of the difficulty, we treat here the schemes producing less neutrons. As for advanced reactors of next generation, catalyzed D- D [1,2] and D- ^3He [3,4] fusion reactors with high temperature are considered. In cases of the former and latter schemes, the ratio of neutron energy to the fusion energy are 30 - 35 % and 3 - 5 %, respectively.

In this paper, we propose innovative schemes of direct energy conversion from the fusion energy to electricity and fuel hydrogen gas in order to apply to the fusion reactor power plant. A new concept of direct energy conversion from synchrotron radiation to electricity using "rectena" (solid-state rectifying antenna receiving high frequency wave beginning at over 2500 GHz) was proposed by Kulcinski et al. in case of APOLLO D - ^3He fusion reactor [3]. This conversion scheme is related with the high temperature (58 keV) in the high magnetic field (19.3 T). In this case, the energy of synchrotron radiation is about 50 % of the fusion power. In contrast to this, here, we mainly study the case of the high temperature (up to 100 keV) but the relatively low magnetic field in the range of 5 -7 T (thus high β) especially for D - ^3He scheme, where the energy of synchrotron radiation is negligibly small (less than 0.3 % at extremely high β). Therefore, in this article, we study direct electron-hole pair production from radiation (DEHPRA) with utilizing semiconductor, that is, bolometric radiation power from the plasma is used to produce directly current or hydrogen (deuterium) gas. The principle of the latter one is based on the electrolysis of water with a semiconductor. The indirect hydrogen production by electrolysis of water with produced electricity can be also utilized for the purpose of flexible energy storage.

II. REACTOR CONSIDERATION

As described in Introduction, the high temperature (up to 100 keV) and high β (thus, relatively low magnetic field in the range of 5 -7 T) plasma is mainly treated for a fusion rector. For this purpose, D-^{3}He as well as catalyzed D-D schemes for fuel seem to be most plausible. The conceptual power flow chart for D-^{3}He fuel scheme is considered here. The main power outputs are P_p by 14.7 MeV protons, P_{br} by bremsstrahlung, and P_{cf} by hot fuel ions flowing out from the confining region. P_n by neutrons and P_{sy} by synchrotron radiation are relatively small. These power outputs are converted mainly to electricity and partly to hydrogen gas as will be described in the next section.

The Bremsstrahlung radiation spectra from high temperature plasma (T_e of less than 0.3 MeV) including relativistic effect are given by Maxon [5]. In Fig.1, the data given in Reference [5] and their best-fit curve are shown for T_e = 100 KeV. Here, the average charge state of ions, Z, is assumed to be 1. This best-fit curve is used hereafter for calculation of γ-ray deposition in the material.

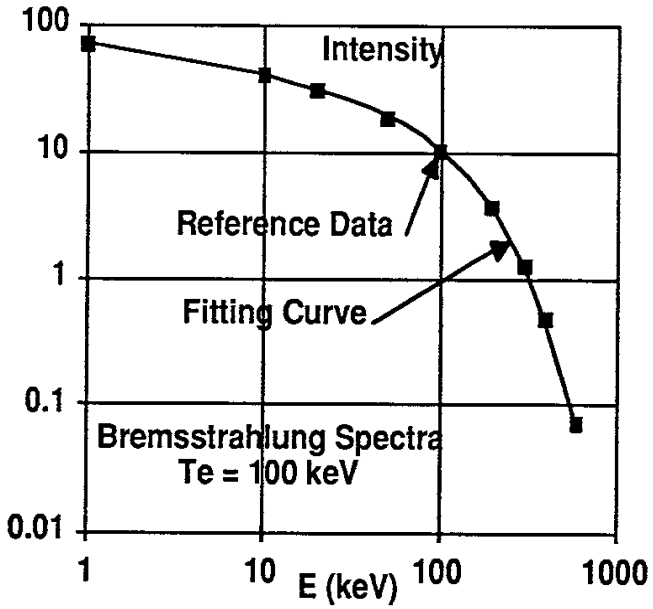

Fig.1 Bremsstrahlung radiation spectra data points given in reference [5] and the best-fit curve.

III. CONCEPTS OF DIRECT HYDROGEN PRODUCTION

The well known device to utilize the radiation energy from the sun is a solar battery, which is typically made of p-n junction of silicon semiconductors. If the light having energy more than the band gap energy is illuminated on the semiconductor, electron-hole pair(s) are produced in the region of the p-n junction. This can cause current, and, thus, the electric power.

Unfortunately, due to the low equivalent temperature spectrum of the sun light, the available photons are limited. Thus, the efficiency is quite low. In contrast to this, the spectrum of the radiation from the fusion plasma has a much higher equivalent temperature. Then, the available photons to produce electron-hole pairs are abundant. So, the radiation from the fusion plasma may efficiently induce current in the semiconductor.

On the other hand, Fujishima and Honda found that only a p-type or n-type semiconductor such as TiO_2 illuminated by photons having more than certain energy can be used directly for electrolysis of water [6]. The process has been well explained with energy band configuration of a semiconductor immersed in the liquid electrolyte. For example, the process for TiO_2 can be considered as follows:

$$TiO_2 + h\nu \rightarrow e^- + p^+$$
$$H_2O + 2p^+ \rightarrow 1/2O_2 + 2H^+ \quad \text{(at } TiO_2 \text{ electrode)}$$
$$2H^+ + 2e^- \rightarrow H_2 \quad \text{(at Pt electrode)}$$

The energy level of the conduction (and also valence) band E_{CB} increases near the surface of semiconductor TiO_2 facing the liquid electrolyte. If the photon having energy larger than the band gap energy ε_g of the semiconductor (ε_g = 3 eV in case of TiO_2) is illuminated on the semiconductor, electron-hole pair(s) are produced, and the electron(s) excited into the conduction band moves the opposite direction to the surface of the semiconductor facing the liquid electrolyte, while the hole in the valence band E_{CV} moves to the surface of the semiconductor facing the liquid electrolyte. Thus, if the semiconductor is connected to the other electrode also immersed in the liquid electrolyte with a conducting wire, electrolysis of water can occur: oxygen gas appears at the TiO_2 surface, and hydrogen gas appears at the other electrode as shown in Fig. 2, where the membrane to separate hydrogen and oxygen gases is not shown for simplicity.

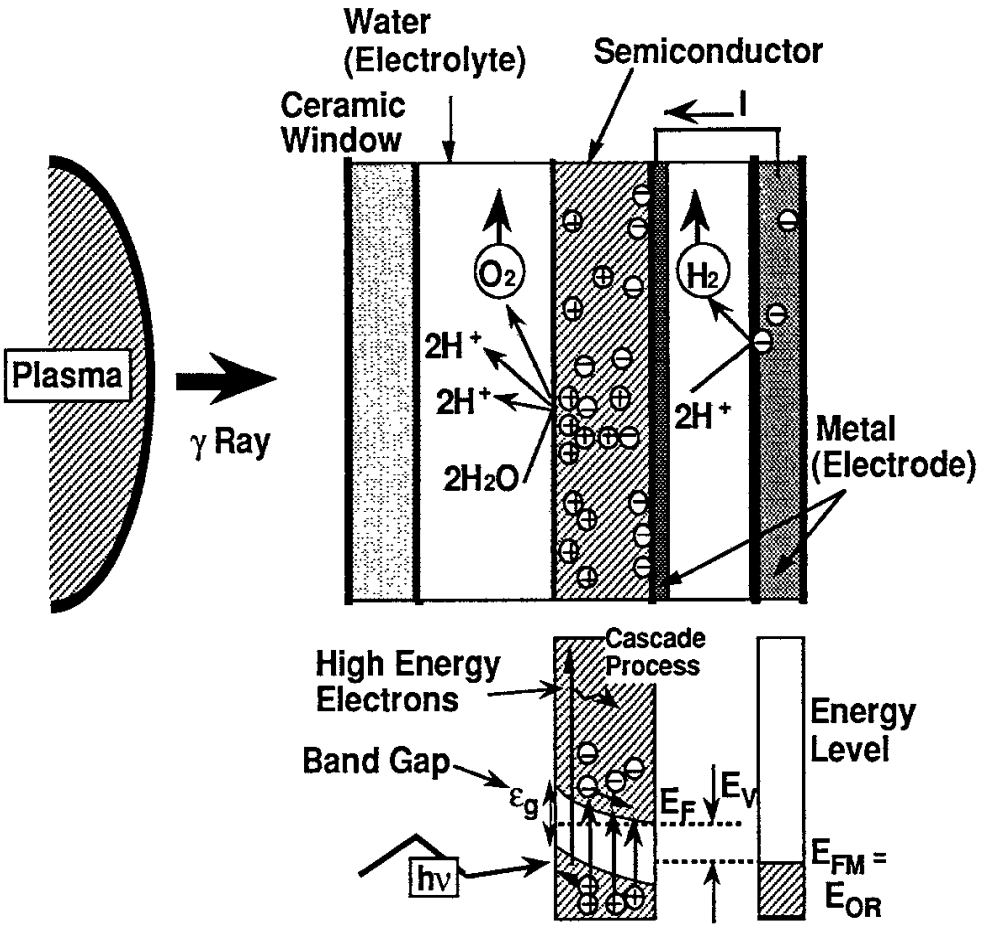

Fig. 2 Principle of direct hydrogen production by γ rays.

The symbols of E_F and E_{FM} are the Fermi energy levels of the semiconductor and the metal electrode, respectively. In the equilibrium state, E_{FM} becomes equal to E_{OR}, where E_{OR} denotes oxidation-reduction potential of the electrode immersed in the liquid electrolyte. Thus, the potential difference, $E_V = E_F - E_{OR}$, appears, and then, the current occurs in this system.

In some type of reactors, there are abundant photons. These photons might be used for direct electrolysis of water without using a turbine generator. One of candidates of primary energy source for efficient H_2 production is γ-ray, because γ-ray has ability to penetrate the material (of the window, for example) rather well. For this purpose, a high temperature reactor such as an advanced D-^{3}He reactor is adequate.

Here, a reactor plasma with temperature of 100 keV is assumed for model calculation, where a ceramic window (such as Si_3N_4) is taken as a first wall. Absorption of γ-ray in the material can be calculated by the following simple formula:

$$I / I_0 = \exp\{-(\mu / \rho)\rho t\}$$

where I is the intensity of γ-ray at some position in the material, and I_0 is the initial intensity of γ-ray, and μ / ρ is mass attenuation coefficient, and ρt is mass thickness. In case of compound, μ / ρ is:

$$\mu / \rho = \Sigma_i W_i (\mu / \rho)_i$$

where W_i is the weight fraction of i th element in the compound or mixture [7]. The photoelectric, total absorption, and total cross sections (the last incudes scattering cross sections) of γ ray in titanium are given by Storm and Israel [8].

Then, mass attenuation coefficient μ / ρ can be calculated. Some of mass attenuation coefficients for the relevant materials are shown in Fig.3.

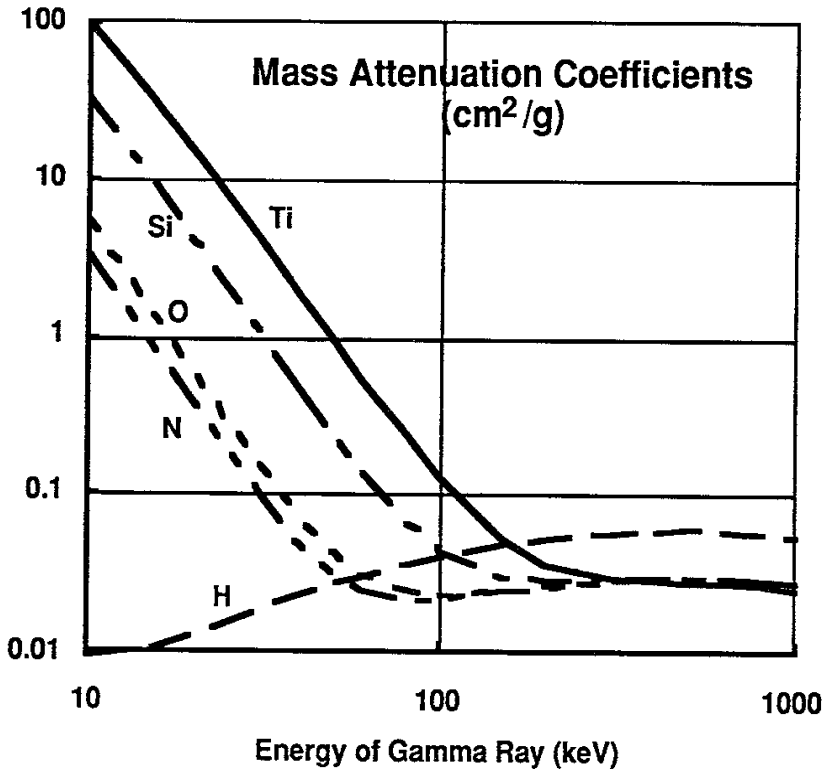

Fig.3 Mass attenuation coefficients for the relevant materials.

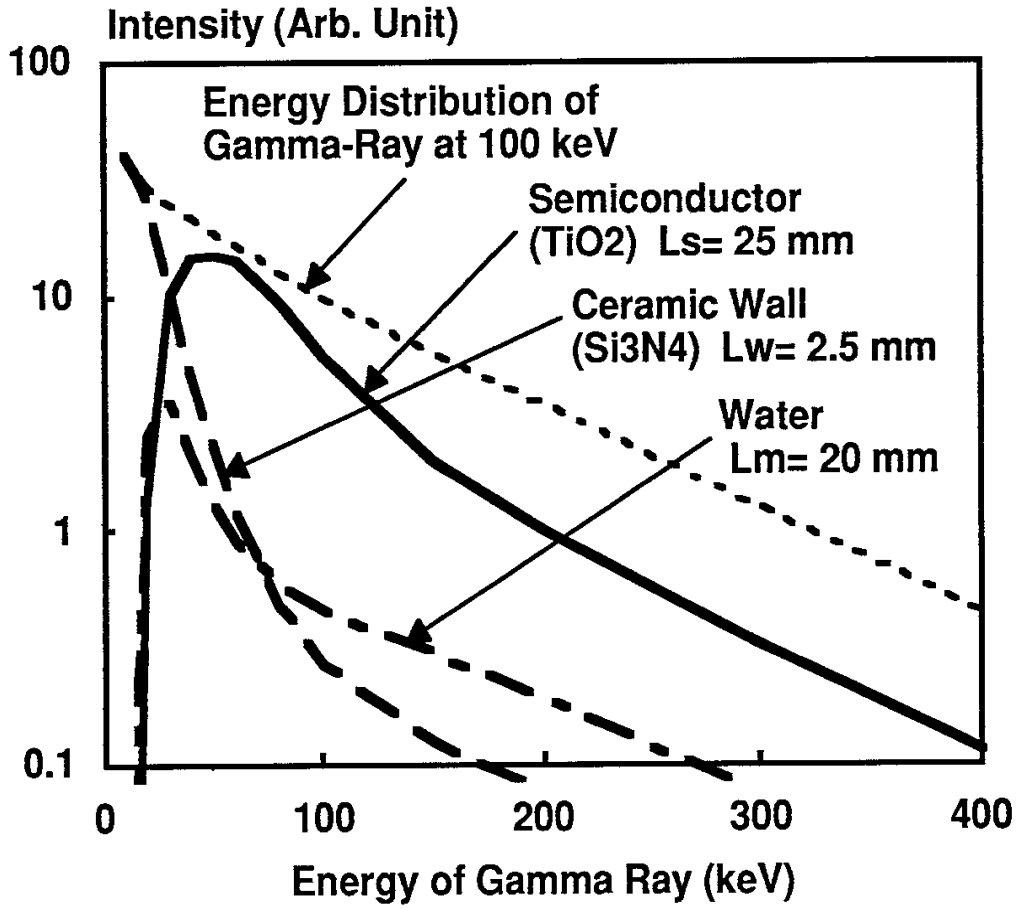

Fig.4 Absorption fraction of γ ray energy in the materials.

Taking energy distribution of emitted photons, absorption fraction of γ ray energy in the materials are shown in Fig.4. From the figure, 37 % of the total energy is absorbed by the first wall of ceramic (Si_3N_4) with thickness of 2.5 mm, while 38 % is absorbed by the semiconductor (such as TiO_2) with effective thickness of 25 mm immersed in the water.

The energy deposition calculation is rather simple, while the configuration of multi-layer of the semiconductor is expected depending on the depletion layer thickness of the semiconductor. If the part of the 1st wall would work as a semiconductor, then the efficiency will be rather improved. We suppose one unit of pipe with outer diameter of 50 mm, and about three layers of such pipes inside the vacuum chamber as shown in Fig. 5. The absorbed power fraction by the TiO_2 semiconductor becomes in total 0.49, while that by the ceramic window is 0.39. The rest is absorbed in the water and the thin Be electrode.

For estimating conversion efficiency, "radiation ionization energy" ε_i (eV) defined as the average energy required to form one electron-hole pair in semiconductor materials is a useful concept:

$$\varepsilon_i = c_0 \varepsilon_g + c_1$$

where c_0 and c_1 are constants, experimentally obtained as 14/5 and 0.5 - 1.0 (eV), respectively [9]. These two constants are fortunately independent from the form of energy source, that is, applicable all to alpha particles, electrons, and photons. Then, we can estimate the production rate $\dot{N}_{eh}$ of electron-hole pairs:

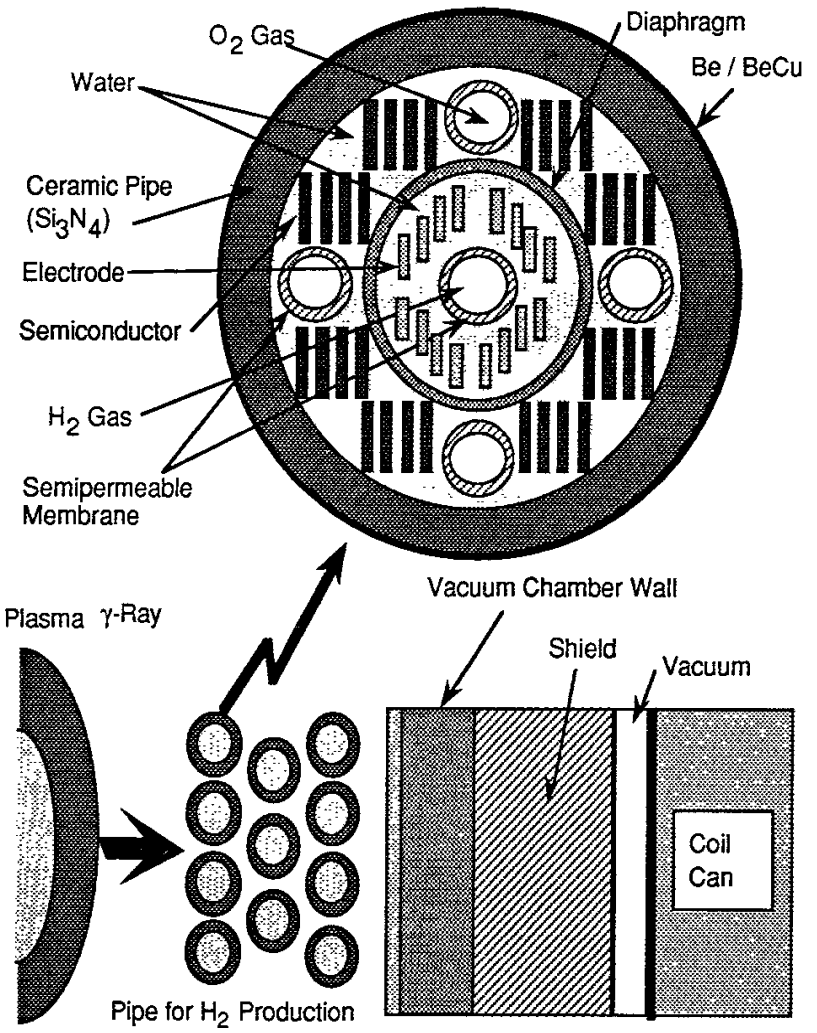

Fig.5 Basic configuration of direct hydrogen production system.

$$\dot{N}_{eh} = \eta_s \eta_w \eta_m P_{br} / e\varepsilon_i$$

where η_s, η_w, and η_m are ratio of available surface area to the vacuum chamber wall, transparency of photons through the first wall, and efficiency of deposition of photon energy on the semiconductors, respectively. If the produced electron-hole pairs are used as a simple battery, the produced electric power P_{sem} is given as follows:

$$\begin{aligned} P_{sem} &= E_V e \dot{N}_{eh} \\ &= \eta_s \eta_w \eta_m P_{br} (E_V / \varepsilon_g) / (c_0 + c_1 / \varepsilon_g) \end{aligned}$$

Thus, the efficiency η_{sem} of direct current production by photons in the semiconductor is given as:

$$\eta_{sem} = \eta_s \eta_w \eta_m (E_V / \varepsilon_g) / (c_0 + c_1 / \varepsilon_g)$$

In case of direct hydrogen production, the above electron-hole pairs are used for electrolysis of water. The production rate N_{hyd} of hydrogen gas is given as:

$$\dot{N}_{hyd} = e\dot{N}_{eh}/(2F)$$

where F is Faraday constant (9.65×10^4 C/mol). Thus, the expected power P_{hb} by burning the hydrogen gas (with oxygen gas) as fuel becomes:

$$P_{hb} = \Delta H_f \dot{N}_{hyd}$$

where ΔH_f is the enthalpy change by burning hydrogen gas (285.8 kJ/mol at 298 K). Then, the efficiency η_{hyd} of direct hydrogen production by photons in the semiconductor is given as:

$$\eta_{hyd} = P_{hb}/P_{br} = \eta_s\eta_w\eta_m\Delta H_f/(2F\varepsilon_i)$$

Then, we get the ratio R_{hs}:

$$R_{hs} \equiv \eta_{hyd}/\eta_{sem} = \Delta H_f/(2FE_V) = 1.48/E_V(eV)$$

This result indicates that the direct hydrogen production is preferable, if E_V based on the characteristics of semiconductor is less than 1.48 eV. The main cause limiting efficiency comes from the fact that the ionization energy ε_i is by a factor of about 3 larger than the band gap energy ε_g as described above. Due to this fact, the ultimate efficiency for both η_{sem} and η_{hyd} is limited at about 1/3.

Two cases of the above efficiency are given in Table 1 with the assumed values of the parameters.

Table 1. Efficiency of hydrogen production.

Symbol / Unit	Assumed Values		Meaning of Symbol
	Case A	Case B	
ε_g / eV	3.0	1.5	Band Gap Energy
E_V/ε_g	0.5	0.7	Normalized Available Voltage
η_s	0.85	0.90	Ratio of Available Surface Area
η_w	0.90	0.90	Transparency of 1st Wall
η_m	0.49	0.80	Efficiency of Photon Energy on the Deposition of Semiconductors
Symbol / Unit	Calculated Values		Meaning of Symbol
η_{sem}	0.10	0.14	Efficiency of Direct Current Production by Photons in the Semiconductor
η_{hyd}	0.06	0.18	Efficiency of Direct Hydrogen Production by Photons

In Case A, ε_g and η_m are assumed to be 3.0 eV (such as for TiO_2), 0.49, respectively. Then, the energy conversion ratio η_{sem} becomes 0.10, and the hydrogen production efficiency η_{hyd} is 0.06. In Case B, ε_g and η_m are taken as 1.5 eV, 0.80, respectively. Then, η_{sem} and η_{hyd} are 0.14 and 0.18, respectively. Thus, the direct hydrogen production is favorable in Case B. It is essential to find appropriate materiel for such a system.

The necessary conditions for the semiconductor adequate to hydrogen production are:

(1) The semiconductor should not be solvable in the liquid electrolyte. Such material for semiconductor is typically oxide composites,

(2) The energy level of the conduction band should be higher than the hydrogen production potential,

(3) The energy level of the valence band should be lower than the oxidation-reduction potential,

(4) The semiconductor should resist against radiation and high temperature.

If P_{br} is assumed to be 612 MW as will be described for ARTEMIS-L in chapter VI, the hydrogen production rate in Case B becomes 364 mol/sec, which corresponds to 63 ton/day hydrogen production. The rest of radiation energy is converted to heat partly due to phonon excitation in the semiconductor. This heat may be directly converted to electricity with utilizing thermoelectric effects [10].

The merit of direct hydrogen production inside the reactor would be in the following points:

(1) The direct hydrogen production can be combined with direct heat conversion scheme. These two are additive. So, the total efficiency can be improved compared to the conventional turbine type generator,

(2) The cooling water could be used simultaneously as electrolyte,

(3) Without changing photon energy to heat, hydrogen gas can be produced directly. This means the burden of heat on the configuration material might be mitigated.

The degree of the merit depends on the characteristics of the semiconductor material and on the plant configuration.

IV. TECHNICAL CONSIDERATION

First, we check the feasibility of use of Si_3N_4 for the ceramic window, although this material is not unique but only one example among several candidates. In Table 2, the physical property of Si_3N_4 ceramic are shown. The tensile strength is rather high up to about 1100 K.

Table 2 Characteristics of Si_3N_4 ceramic.

Physical property	Unit	Value
Thermal conductivity	W / mm K	2.93×10^{-2}
Specific heat	W / kg K	5.02×10^{2}
Specific gravity	kg/ mm^3	3.2×10^{-6}
Flexural strength	kg / mm^2	1.0×10^{2} at 310 -1070 K
Young's modulus	kg / mm^2	3.1×10^{-4}
Poisson's ratio	-	2.7×10^{-1}
Coefficient of linear expansion	1 / K	2.5×10^{-6} at 310 - 670 K

The heat and stress analyses of the pipe made of Si_3N_4 containing water are carried out. The direction of the heat flux is taken into account. The heat flux q_0 from the plasma is assumed as 2 MW / m^2. The thermal load q_{tp} on the pipe surface is then $q_{tp} = q_0 \sin\theta$, where θ is angular coordinate of the pipe. Two cases are studied; in Case I, the temperature of the cooling water is assumed to be 573 K at inlet and 603 K at outlet, and in Case II, 413 K at inlet and 443 K at outlet. The former case is favorable to the second use of the thermal energy, for example, with thermoelectric effects in the semiconductor. The latter is adequate for applying the existing membrane to separate the hydrogen and oxygen gases, because well established polymer membranes would be used under the relatively low temperature. The fluid velocity is adjusted to keep the above temperature difference. The pipe length is 5 m in both Cases. The pressure is taken as 15 MPa in Case I. These analyses show the Si_3N_4 ceramic pipe with diameter of 50 mm and thickness of 2.5 mm (as shown in Fig.5) should be able to withstand both the thermal stress and internal pressure (28.2 kg / mm^2 in total for fluid velocity of 1.82 m/s). The effects of fluid velocity on temperature and tensile strength of the pipe are shown in Fig.6.

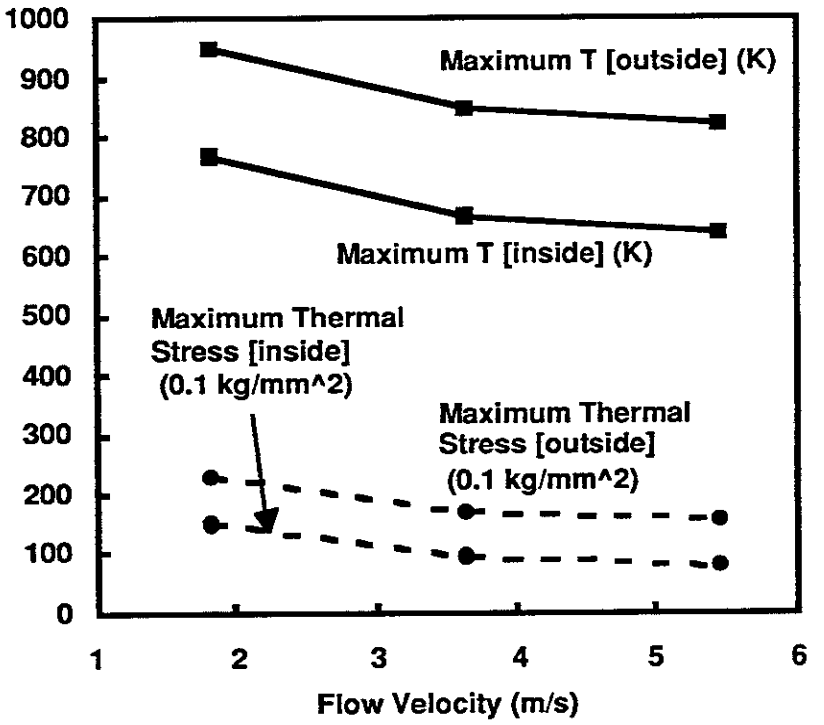

Fig.6 Effects of fluid velocity on temperature and stress of the pipe for direct hydrogen production.

The new scheme of a fusion reactor system involving the above concept without a turbine generator seems favorable as an advanced reactor of next generation such as innovative catalyzed D- D or D- ^3He fusion reactors with high temperature. One of candidates for the D- ^3He reactor concept is FRC (Field-Reversed Configuration, a typical design is ARTEMIS-L [4, 11-13]).

In case of 1 GW electricity output for ARTEMIS-L, the power flow is shown in Fig. 7. As shown in Fig. 7, the indirect hydrogen gas production through the electrolysis with produced electricity can be also used for energy reservoir. If the needs of electricity becomes low in night for example, the excessive electric power can be stored in the form of hydrogen gas. The efficiency of electrolysis of water is rather high (more than 90 %) within the present state of art.

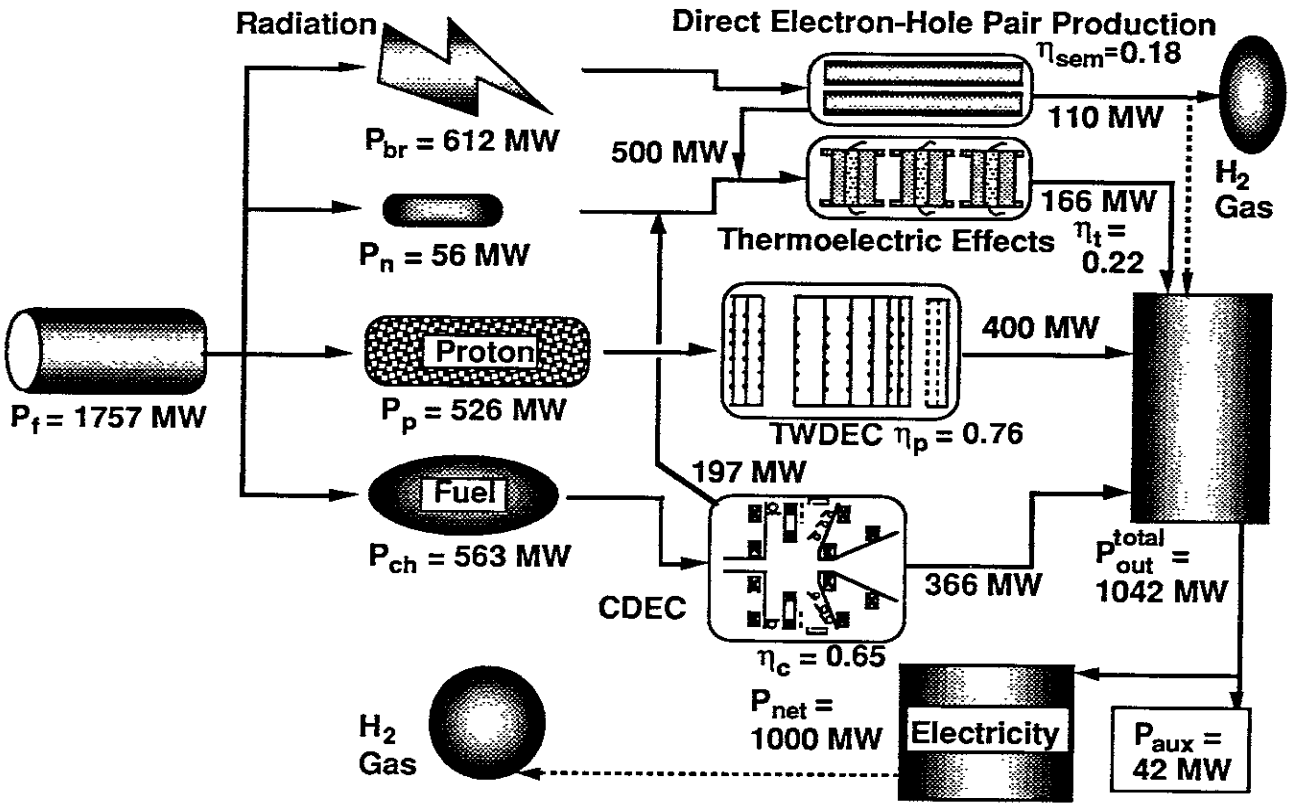

Fig. 7 Power flow for ARTEMIS-L having 1 GW electricity output.

V. CONCLUSION

As one of methods of innovative energy production in fusion reactors without having a conventional turbine-type generator, an efficient use of radiation produced in a fusion reactor with utilizing semiconductor and supplying clean fuel in a form of hydrogen gas are proposed. Taking the candidates of reactors for application of the new concept, the expected efficiency is estimated. Furthermore, the power flow is preliminarily studied.

ACKNOWLEDGMENT

The authors acknowledge Dr. T. Kato for information about interaction between photons and materials, and Dr. M. Sasao about interaction between neutrons and materials.

REFERENCES

[1] K. Evans, C. C. Baker, et al., Nucl. Technology / Fusion 4(1983)226.

[2] A. Iiyoshi, O. Motojima, et al., in Proc. of 7th Symp. on Engineering Problems on Fusion Research, Knoxville, U.S.A., (1977)1683.

[3] G. L. Kulcinski, G. A. Emmert, et al., Fusion Technology, **15**(1989)1233.

[4] H. Momota, A. Ishida, et al., Fusion Technology, **21**(1992)2307.

[5] S. Maxon, Phys. Rev. A, **5**(1972)1630.

[6] A. Fujishima and K. Honda, Nature, **238**(1972)37.

[7] G.F. Knoll, in "Radiation detection and measurement" John Willey & Sons, Inc., New York (1979).

[8] E. Storm and H.I. Israel, Nucl. Data Tables, A7(1970)565.
[9] C. A. Klein, Jour. Appl. Phys. **39**(1968)2029.
[10] S. Yamaguchi, et al, ICENES'93, Makuhari, Japan, 1993, (BP-25).
[11] A. Iiyoshi, et al, ICENES'93, Makuhari, Japan, 1993, (O-6).
[12] H. Momota, et al, ICENES'93, Makuhari, Japan, 1993, (AP-46).
[13] H. Tomita, et al, ICENES'93, Makuhari, Japan, 1993, (AP-47).

Recent Issues of NIFS Series

NIFS-199 M. Tanaka, *A Kinetic Simulation of Low-Frequency Electromagnetic Phenomena in Inhomogeneous Plasmas of Three-Dimensions* ; Nov. 1992

NIFS-200 K. Itoh, S.-I. Itoh, H. Sanuki and A. Fukuyama, *Roles of Electric Field on Toroidal Magnetic Confinement*, Nov. 1992

NIFS-201 G. Gnudi and T. Hatori, *Hamiltonian for the Toroidal Helical Magnetic Field Lines in the Vacuum*; Nov. 1992

NIFS-202 K. Itoh, S.-I. Itoh and A. Fukuyama, *Physics of Transport Phenomena in Magnetic Confinement Plasmas*; Dec. 1992

NIFS-203 Y. Hamada, Y. Kawasumi, H. Iguchi, A. Fujisawa, Y. Abe and M. Takahashi, *Mesh Effect in a Parallel Plate Analyzer*; Dec. 1992

NIFS-204 T. Okada and H. Tazawa, *Two-Stream Instability for a Light Ion Beam -Plasma System with External Magnetic Field;* Dec. 1992

NIFS-205 M. Osakabe, S. Itoh, Y. Gotoh, M. Sasao and J. Fujita, *A Compact Neutron Counter Telescope with Thick Radiator (Cotetra) for Fusion Experiment*; Jan. 1993

NIFS-206 T. Yabe and F. Xiao, *Tracking Sharp Interface of Two Fluids by the CIP (Cubic-Interpolated Propagation) Scheme*, Jan. 1993

NIFS-207 A. Kageyama, K. Watanabe and T. Sato, *Simulation Study of MHD Dynamo : Convection in a Rotating Spherical Shell*; Feb. 1993

NIFS-208 M. Okamoto and S. Murakami, *Plasma Heating in Toroidal Systems*; Feb. 1993

NIFS-209 K. Masai, *Density Dependence of Line Intensities and Application to Plasma Diagnostics*; Feb. 1993

NIFS-210 K. Ohkubo, M. Hosokawa, S. Kubo, M. Sato, Y. Takita and T. Kuroda, *R&D of Transmission Lines for ECH System* ; Feb. 1993

NIFS-211 A. A. Shishkin, K. Y. Watanabe, K. Yamazaki, O. Motojima, D. L. Grekov, M. S. Smirnova and A. V. Zolotukhin, *Some Features of Particle Orbit Behavior in LHD Configurations*; Mar. 1993

NIFS-212 Y. Kondoh, Y. Hosaka and J.-L. Liang, *Demonstration for Novel Self-organization Theory by Three-Dimensional Magnetohydrodynamic Simulation*; Mar. 1993

NIFS-213 K. Itoh, H. Sanuki and S.-I. Itoh, *Thermal and Electric Oscillation Driven by Orbit Loss in Helical Systems*; Mar. 1993

NIFS-214 T. Yamagishi, *Effect of Continuous Eigenvalue Spectrum on Plasma Transport in Toroidal Systems*; Mar. 1993

NIFS-215 K. Ida, K. Itoh, S.-I.Itoh, Y. Miura, JFT-2M Group and A. Fukuyama, *Thickness of the Layer of Strong Radial Electric Field in JFT-2M H-mode Plasmas*; Apr. 1993

NIFS-216 M. Yagi, K. Itoh, S.-I. Itoh, A. Fukuyama and M. Azumi, *Analysis of Current Diffusive Ballooning Mode*; Apr. 1993

NIFS-217 J. Guasp, K. Yamazaki and O. Motojima, *Particle Orbit Analysis for LHD Helical Axis Configurations* ; Apr. 1993

NIFS-218 T. Yabe, T. Ito and M. Okazaki, *Holography Machine HORN-1 for Computer-aided Retrieve of Virtual Three-dimensional Image* ; Apr. 1993

NIFS-219 K. Itoh, S.-I. Itoh, A. Fukuyama, M. Yagi and M. Azumi, *Self-sustained Turbulence and L-Mode Confinement in Toroidal Plasmas* ; Apr. 1993

NIFS-220 T. Watari, R. Kumazawa, T. Mutoh, T. Seki, K. Nishimura and F. Shimpo, *Applications of Non-resonant RF Forces to Improvement of Tokamak Reactor Performances Part I: Application of Ponderomotive Force* ; May 1993

NIFS-221 S.-I. Itoh, K. Itoh, and A. Fukuyama, *ELMy-H mode as Limit Cycle and Transient Responses of H-modes in Tokamaks* ; May 1993

NIFS-222 H. Hojo, M. Inutake, M. Ichimura, R. Katsumata and T. Watanabe, *Interchange Stability Criteria for Anisotropic Central-Cell Plasmas in the Tandem Mirror GAMMA 10 ;* May 1993

NIFS-223 K. Itoh, S.-I. Itoh, M. Yagi, A. Fukuyama and M. Azumi, *Theory of Pseudo-Classical Confinement and Transmutation to L-Mode;* May 1993

NIFS-224 M. Tanaka, *HIDENEK: An Implicit Particle Simulation of Kinetic-MHD Phenomena in Three-Dimensional Plasmas;* May 1993

NIFS-225 H. Hojo and T. Hatori, *Bounce Resonance Heating and Transport in a Magnetic Mirror;* May 1993

NIFS-226 S.-I. Iton, K. Itoh, A. Fukuyama, M. Yagi, *Theory of Anomalous Transport in H-Mode Plasmas;* May 1993

NIFS-227 T. Yamagishi, *Anomalous Cross Field Flux in CHS* ; May 1993

NIFS-228 Y. Ohkouchi, S. Sasaki, S. Takamura, T. Kato, *Effective Emission and Ionization Rate Coefficients of Atomic Carbons in Plasmas;* June 1993

NIFS-229 K. Itoh, M. Yagi, A. Fukuyama, S.-I. Itoh and M. Azumi, *Comment on 'A Mean Field Ohm's Law for Collisionless Plasmas;* June 1993

NIFS-230 H. Idei, K. Ida, H. Sanuki, H. Yamada, H. Iguchi, S. Kubo, R. Akiyama, H. Arimoto, M. Fujiwara, M. Hosokawa, K. Matsuoka, S. Morita, K. Nishimura, K. Ohkubo, S. Okamura, S. Sakakibara, C. Takahashi, Y. Takita, K. Tsumori and I. Yamada, *Transition of Radial Electric Field by Electron Cyclotron Heating in Stellarator Plasmas;* June 1993

NIFS-231 H.J. Gardner and K. Ichiguchi, *Free-Boundary Equilibrium Studies for the Large Helical Device,* June 1993

NIFS-232 K. Itoh, S.-I. Itoh, A. Fukuyama, H. Sanuki and M. Yagi, *Confinement Improvement in H-Mode-Like Plasmas in Helical Systems,* June 1993

NIFS-233 R. Horiuchi and T. Sato, *Collisionless Driven Magnetic Reconnection,* June 1993

NIFS-234 K. Itoh, S.-I. Itoh, A. Fukuyama, M. Yagi and M. *Azumi, Prandtl Number of Toroidal Plasmas;* June 1993

NIFS-235 S. Kawata, S. Kato and S. Kiyokawa , *Screening Constants for Plasma;* June 1993

NIFS-236 A. Fujisawa and Y. Hamada, *Theoretical Study of Cylindrical Energy Analyzers for MeV Range Heavy Ion Beam Probes;* July 1993

NIFS-237 N. Ohyabu, A. Sagara, T. Ono, T. Kawamura and O. Motojima, *Carbon Sheet Pumping;* July 1993

NIFS-238 K. Watanabe, T. Sato and Y. Nakayama, *Q-profile Flattening due to Nonlinear Development of Resistive Kink Mode and Ensuing Fast Crash in Sawtooth Oscillations;* July 1993

NIFS-239 N. Ohyabu, T. Watanabe, Hantao Ji, H. Akao, T. Ono, T. Kawamura, K. Yamazaki, K. Akaishi, N. Inoue, A. Komori, Y. Kubota, N. Noda, A. Sagara, H. Suzuki, O. Motojima, M. Fujiwara, A. Iiyoshi, *LHD Helical Divertor;* July 1993

NIFS-240 Y. Miura, F. Okano, N. Suzuki, M. Mori, K. Hoshino, H. Maeda, T. Takizuka, JFT-2M Group, K. Itoh and S.-I. Itoh, *Ion Heat Pulse*

after Sawtooth Crash in the JFT-2M Tokamak; Aug. 1993

NIFS-241 K. Ida, Y.Miura, T. Matsuda, K. Itoh and JFT-2M Group, *Observation of non Diffusive Term of Toroidal Momentum Transport in the JFT-2M Tokamak;* Aug. 1993

NIFS-242 O.J.W.F. Kardaun, S.-I. Itoh, K. Itoh and J.W.P.F. Kardaun, *Discriminant Analysis to Predict the Occurrence of ELMS in H-Mode Discharges;* Aug. 1993

NIFS-243 K. Itoh, S.-I. Itoh, A. Fukuyama, *Modelling of Transport Phenomena;* Sep. 1993

NIFS-244 J. Todoroki, *Averaged Resistive MHD Equations;* Sep. 1993

NIFS-245 M. Tanaka, *The Origin of Collisionless Dissipation in Magnetic Reconnection;* Sep. 1993

NIFS-246 M. Yagi, K. Itoh, S.-I. Itoh, A. Fukuyama and M. Azumi, *Current Diffusive Ballooning Mode in Seecond Stability Region of Tokamaks;* Sep. 1993

NIFS-247 T. Yamagishi, *Trapped Electron Instabilities due to Electron Temperature Gradient and Anomalous Transport;* Oct. 1993

NIFS-248 Y. Kondoh, *Attractors of Dissipative Structure in Three Disspative Fluids;* Oct. 1993

NIFS-249 S. Murakami, M. Okamoto, N. Nakajima, M. Ohnishi, H. Okada, *Monte Carlo Simulation Study of the ICRF Minority Heating in the Large Helical Device;* Oct. 1993

NIFS-250 A. Iiyoshi, H. Momota, O. Motojima, M. Okamoto, S. Sudo, Y. Tomita, S. Yamaguchi, M. Ohnishi, M. Onozuka, C. Uenosono, *Innovative Energy Production in Fusion Reactors;* Oct. 1993

NIFS-251 H. Momota, O. Motojima, M. Okamoto, S. Sudo, Y. Tomita, S. Yamaguchi, A. Iiyoshi, M. Onozuka, M. Ohnishi, C. Uenosono, *Characteristics of D-^{3}He Fueled FRC Reactor; ARTEMIS-L,* Nov. 1993

NIFS-252 Y. Tomita, L.Y. Shu, H. Momota, *Direct Energy Conversion System for D-^{3}He Fusion;* Nov. 1993